Numerical Characterization of Thermo-mechanical Performance of Breeder Pebble Beds

Zhiyong An, Alice Ying, Mohamed Abdou

PII: S0022-3115(07)00612-5
DOI: 10.1016/j.jnucmat.2007.04.040
Reference: NUMA 42968

To appear in: *Journal of Nuclear Materials*

Cover Page

Paper ID # 45437

Title: Numerical Characterization of Thermo-mechanical Performance of Breeder Pebble Beds

Authors: Zhiyong An*, Alice Y. Ying, Mohamed Abdou

Mechanical & Aerospace Engineering Department, UCLA, Los Angeles, CA 90095-1597

Tel: (310) 794-4452

Fax: (310) 825-2599

E-mail address of the corresponding author: an@fusion.ucla.edu

Numerical Characterization of Thermo-mechanical Performance of Breeder Pebble Beds

Zhiyong An, Alice Ying, and Mohamed Abdou

Mechanical and Aerospace Engineering Dept., UCLA, Los Angeles, CA 90095-1597, USA
an@fusionl.ucla.edu

Abstract

A numerical approach using the discrete element method (DEM) has been applied to study the thermo-mechanical properties of ceramic breeder pebble beds. This numerical scheme is able to predict the inelastic behavior observed in a loading and unloading operation. In addition, it demonstrates that the average value of contact force increases linearly with overall pressure, but at a much faster rate, about 3.4 times the overall pressure increase rate. In this paper, the thermal creep properties of two different ceramic breeder pebble materials, Li_4SiO_4 and Li_2O, are also examined by the current numerical code. The difference found in the properties of candidate materials is reflected numerically in the overall strain in the pebble bed when the stress magnitude becomes smaller.

Key Words: Breeding materials for fusion, thermo-mechanical properties, mathematical and computational method.

1. Introduction

Ceramic breeder pebble bed is an important component in the solid breeder blankets. Practical use of the breeder pebble beds in fusion power reactors requires good characterization of the thermo-mechanical behavior and irradiation effects of the pebble beds. Different from solid materials, mechanical behavior of the pebble beds is not only dependent on the pebble materials, but also related to other parameters (e.g., pebble size, packing density of the pebble bed and bed structure, etc.). Experimental and numerical approaches [1-3] have been tried to quantify the thermo-mechanical characteristics of ceramic breeder pebble beds. According to previous works, ceramic pebble beds show inelastic mechanical behavior, and at elevated temperatures, the pebble bed behavior is affected by thermal creep deformation, especially in the first 10 hours of operation. However, due to the lack of a detailed and insightful description of pebble bed properties, the existing predictive capability mainly based on experimental approaches may not fully quantify their thermo-mechanical state.

A numerical algorithm based on the discrete element method is currently being developed by the UCLA Fusion Science & Technology Center to predict the thermo-mechanical behavior of ceramic breeder pebble beds, particularly in the time-dependent creep deformation regime. In the discrete element method (DEM), each individual particle is separately considered; particles are connected only through contacts by appropriate physics-based interaction laws. As mentioned in a previous paper [4], compared to experimental work, this numerical algorithm can provide more comprehensive information, such as the magnitude of the force at inter-particle contacts, as well as the stress-strain relationships of a pebble bed. With that information, we can obtain information on the likelihood of particle breakage and the thermal conductance at the bed/clad interface.

In this paper, we will exploit the thermo-mechanical properties of ceramic breeder pebble beds with respect to compressive loading at high temperature. For our program, a new inter-particle model, which is based on Hertz-Mindlin's formulation [5], has been updated to include thermal creep deformation. In general, for contacted particles, thermal creep deformation increases contact area and decreases contact stresses. The new microstructural plasticity model describes the creep behavior of contacted particles, which can be easily incorporated into our discrete element program.

2. Algorithm of numerical simulation

In the DEM program, the thermo-mechanical behavior of the ceramic breeder pebble bed can be modeled as a collection of particles interacting via Hertz-Mindlin contact interactions. When the stresses and temperature are high enough, creep deformation needs to be considered. Figure 1 shows two typical particles in contact in a packed pebble bed. The insert figure on the right shows the von Mises stress distribution calculated by finite element analysis (FEA). We can see that stresses are non-uniform and are highly concentrated near the contact. During the simulation, the contact radius, a, is an important parameter for determining the displacement of two particles.

At each contact, a virtual spring is applied to simulate the particle-environment relationship. A contact force can be calculated by the deformation and the stiffness of the virtual spring. The stiffness of the virtual spring, including contact normal and shear stiffness, is determined by the properties of the contacting particles and their deformation. In this code, all ceramic breeder pebbles are assumed to have a spherical shape. The contact force and the stiffness of the contacting pebbles are estimated from Hertz-Mindlin's formulation. The contact force and stiffness will be updated when creep deformation needs to be considered. For each particle, the resultant force and stiffness are directly obtained by summing these properties over all its contacts.

During our simulations, the contacts inside a pebble bed will be determined by particle position and geometry. Between each cycle, the pebble bed is unsteady and the movement of each particle will be calculated by its summed contact force and stiffness. For example, if the resultant force of a particle in the *x*-direction is not equal to zero, there is an incremental displacement in the *x*-direction, which is obtained by dividing the resultant force by the stiffness. In our program, the friction at the contacts is also considered. The following equations are used to determine the movement of particles:

$$\Delta D_x = 0 \qquad \text{for} \quad |\sum_i F_{ix}| \le k_f \sum_i |F_{iy}| \tag{1}$$

Otherwise,

$$\Delta D_x = \frac{\sum_i F_{ix} - k_f \sum_i |F_{iy}|}{k_x} \tag{2}$$

where $k_f = tan\phi \cdot \mu$ is the friction coefficient at contacts and k_x is the resultant stiffness in *x*-direction.

At high stresses and elevated temperatures, creep deformation will affect the normal and friction forces at the contact. In particular, contact stresses will be relaxed due to contact neck increase. In general, creep deformation for materials can be evaluated by power-law creep:

$$\dot{\varepsilon}_c = c\sigma^n \tag{3}$$

where the coefficient *c* is dependent on material properties and temperature, c is the von Mises stress in MPa, *n* is the stress exponent and $\dot{\varepsilon}$ is the creep rate in s^{-1}. In the literature [6, 7], a stress exponent of around 3.6±0.5 was found for Li_2O in the temperature range of 700-800^{o}C and stress range of 15-45MPa. For 90% dense Li_4SiO_4, the stress exponent is about 3.6±0.2 with a temperature around 850^{o}C and the stress range is about 50-200MPa.

In our numerical program, it is assumed that the rate of increase in contact radius due to creep deformation is on the same order as the shrinkage rate of the two contacting particles. As shown in Figure 1, for two contacting particles, high stresses are concentrated at the contact area. Under Hertz-Mindlin's contact theory, the maximum stress is located at about 0.57*a* from the contact interface, where *a* is the radius of the contact circle. According to the geometry of two contacting spheres, the power-law creep deformation will affect the contact area as shown in the following equation:

$$\dot{\varepsilon}_{oc} = \alpha \, \dot{\varepsilon}_a \tag{4}$$

where $\alpha = 0.57a$. And in the above equation, $\dot{\varepsilon}_a$ can be obtained by solving:

$$\alpha \left(\dot{\varepsilon}_a t\right)\left(1+\dot{\varepsilon}_a t\right)^{2n} = c\, t \left(\frac{p}{\pi a_0^2}\right)^n \tag{5}$$

where *t* is creep time and a_0 is the initial value of the contact radius. Figure 2 shows the local contact creep deformation model for particle material with $c = 10^{-17}$ and $n = 4.0$. The above equation is in good agreement with the finite element analysis result, where creep deformation is calculated for two particles. The above creep model is derived from two perfect contacting spherical particles, without any breaking during deformation. For non-spherical particles, the mass involved with creep deformation is difficult to calculate, however, a contact circle with the same area size can be equivalent to an irregular contact area. Further study needs to specify the coefficient in Eq. (4).

3. Mechanical properties of pebble beds

Fundamental mechanical properties of lithium ceramics have been obtained from previous experiments. However, after a lithium ceramic is packed in the form of a pebble bed, its mechanical properties are much different from its properties as a bulk material. Based on experimental results, Reimann et al. [1] provided the effective mechanical properties of ceramic breeder pebble beds. The effective constitutive equations derived from these experiments show a nonlinear behavior of the macroscopic stress-strain relation. As they are based on a continuous model, no detail can be derived on "particle" quantity like the deterministic way whether or not the particle is under stress high enough for creep deformation.

Figure 3 shows the stress-strain response of a ceramic pebble bed with Li_4SiO_4 breeder materials. The small figure shows the geometry of the tested pebble bed. First, numerical results show that the mechanical behavior of a pebble bed system is inelastic, and the stiffness of a pebble bed is dependent on applied loading. Second, the results show that irreversible pebble displacement is generated after one loading-unloading cycle. This is a plastic-like behavior of particular materials. In other tests, it has been found that this property is related to bed packing properties such as packing density, particle size distribution, geometry of the pebble bed container, etc. For fusion blanket design, vibration packing is an important process to achieve consistent experimental results in order to eliminate or minimize this effect.

One advantage of discrete element analysis is that information about pebble-to-pebble contacts inside the pebble beds can be obtained through calculation. Figure 4 shows the distribution of contact force under different loads. The contact forces inside the pebble bed increase significantly with loading. The insert figure shows that the rate of increase in the average contact force value is about 3.4 times the rate of increase of the applied pressure. Based on this information, breeder structure loads can be designed to prevent exceeding the crush force of breeder pebbles.

4. Analysis of creep deformation

Creep deformation under constant thermal deformation is more typical for fusion blanket design. Under compression, deformation will increase the contact area between particles and reduce the thermal stresses generated inside the pebble beds. On the other hand, when the breeding blanket is exposed to a pulsed irradiation environmnet, the creep deformation will cause a total volume loss in the pebble beds and may generate some gaps between the pebble beds and the structure container, which potentially can cause the breeder material to exceed its operating temperature limit and endanger the operation of the fusion reactor.

In previous experiments and numerical simulations [1, 3], the creep deformation has been observed to exist in a pebble bed when the temperature is sufficiently high. In this paper, the relation between the creep strain rate of materials in bulk and pebble bed form will be explored. Our DEM simulation code was applied to two different breeder materials, Li_4SiO_4 and Li_2O. The mechanical properties are listed in Table 1.

Figure 5 shows the code prevision for the axial creep strain and strain rate of Li_4SiO_4 and Li_2O pebble beds under uniaxial pressure, when the temperature is about 850^oC. The pressure applied in this calculation is about 10MPa on the top and bottom surfaces. The two of the lines show that the creep strains of pebble beds with different breeder materials are similar during the first three hours, but the Li_2O pebble bed shows a larger creep strain after three hours. Two data points in Figure 5 show the creep strain rates of the same two pebble beds; there is not much difference between them. Similar to experimental results, numerical data of both ceramic breeder pebble beds show that the creep strain rate decreases over time, even though the load remains constant. When considering the load on a pebble bed as equivalent to the pressure on a bulk material, the strain rate of a pebble bed is much higher than that of solid material. This means that contact stresses concentrated near the contact areas can enhance the creep deformation of materials.

5. Conclusion

The current numerical approach will help us to better understand the thermo-mechanical properties and characteristics of ceramic breeder pebble beds. As revealed in the analysis, it is particularly exciting that the contact force at particle/particle contacts can be correlated with the external applied pressure. Our approach provides a flexible method to predict the mechanical performance of breeder pebble beds under different temperature or boundary conditions, as well as thermal creep deformation. Numerical results of two different ceramic breeder pebble materials, Li_4SiO_4 and Li_2O, show that the creep strain rate of pebble beds are higher than bulk materials at steady state, while the difference between different pebble beds thermal creep magnitude is less significant than the difference between pebble beds and the bulk material. In the future, more complex cases, including thermal expansion and tri-axial loading, will be developed to examine the coupled thermo-mechanical behavior of ceramic breeder pebble beds.

Acknowledgement

This work was performed under U. S. Department of Energy Contract DE-FG03-ER52123.

References

[1] J. Reimann, J. Boccaccini, M. Enoeda and A.Y. Ying, Thermomechanics of solid breeder and Be pebble bed materials, Fusion Engineering and Design, 61-62 (2002) 319-331.

[2] L. Bühler, Continuum models for pebble beds in fusion blankets, FZKA 6561, 2002.

[3] Z. An, A. Ying and M. Abdou, "Experimental & numerical study of ceramic breeder pebble bed thermal deformation behavior", Fusion Science and Technology, 47 (4) (2005) 1101-1105.

[4] Z. An, A. Ying and M. Abdou, "Assessment of Discrete Element Method for Ceramic Breeder Pebble Beds Thermo-mechanical Performances Characterization", Seventh International Symposium on Fusion Nuclear Technology, Tokyo, Japan, May 22-27, 2005.

[5] R.D. Mindlin, "Microstructure in linear elasticity", Archive for Rational Mechanisms and Analysis 16 (1969) 51-78.

[6] M.C. Billone, Y.Y. Liu, R.B. Poeppel, J.L. Routbort, K.C. Goretta, D.S. Kupperman, "Elastic and Creep Properities of Li_2O", J. Nuclear Material, 141-143 (1986) 282-288.

[7] C-Y. Chu, K. Bar, J.P. Singh, K.C. Goretta, M.C. Billone, R.B. Poeppel, and J.L. Routbort, "Mechanical properties of polycrystalline lithium orthosilicate", J. Am. Ceram. Soc., 72 (9) (1989) 1643-48.

Table Caption

Table 1 Summary of material properties of Lithium ceramic breeder materials

	E (GPa)	μ (GPa)	*K* (GPa)	Poisson ratio (ν)	Constant coefficient (*c* in Eq.3)	Stress component (*n* in Eq.3)
Li_4SiO_4	138	55.4	68.8	0.25	5.2×10^{-13}	3.6
Li_2O	141	60.3	75.8	0.19	9.277×10^{-11}	3.6

Figure Caption

Figure 1 Sketch of two contacting particles. (The right-insert figure shows a FEA simulation and light color areas stand for the highest stress.)

Figure 2 Verification of DEM creep model compared with FEA simulation of two particles.

Figure 3 Stress-strain behavior of a rectangular pebble bed under uniaxial pressure (along *y*-direction).

Figure 4 Evolution of contact force magnitude during increasing loading process.

Figure 5 Axial creep strain and strain rate of Li_4SiO_4 and Li_2O pebble beds under uniaxial pressure (P = 10MPa).

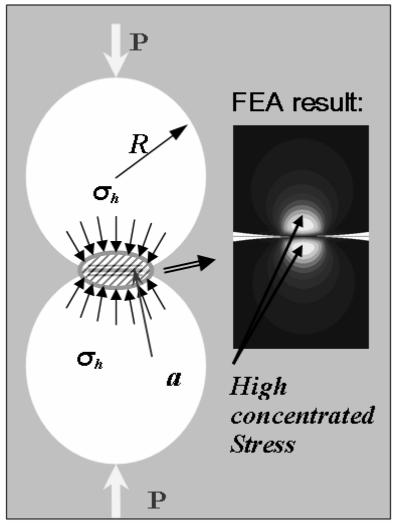

Figure 1 Sketch of two contacting particles. (The right insert figure shows a FEA simulation and light color areas stand for the highest stress.)

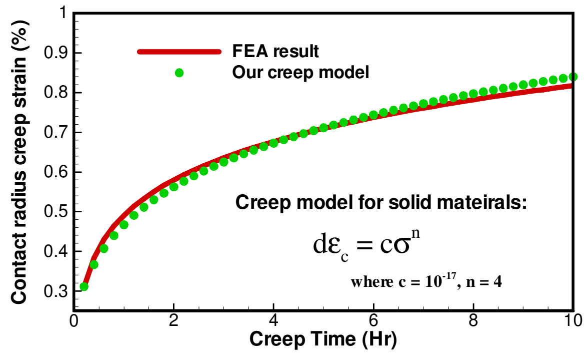

Figure 2 Verification of DEM creep model compared with FEA simulation of two particles.

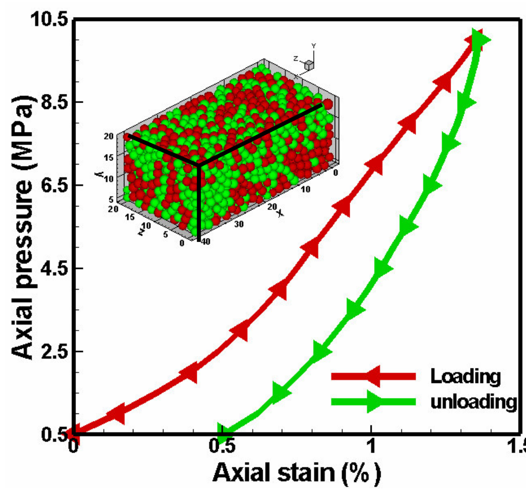

Figure 3 Stress-strain behavior of a rectangular pebble bed under uniaxial pressure (along *y*-direction).

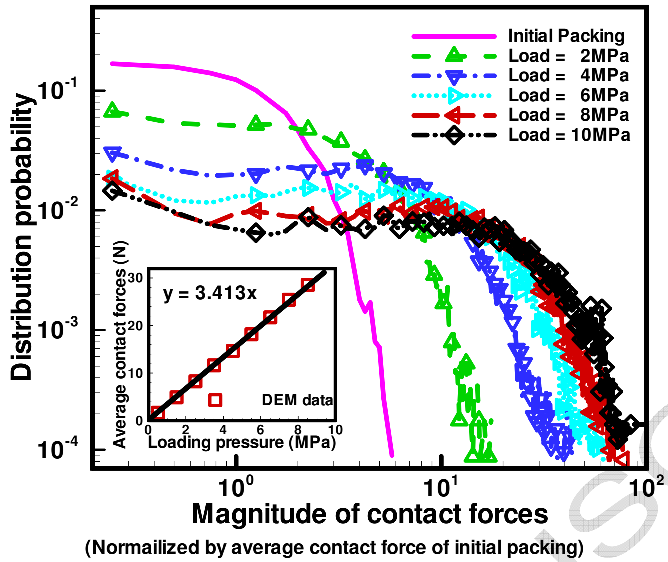

Figure 4 Distribution of particle contact force as a function of applied load. (The insert figure shows the magnitude relationship between average contact force and overall pressure.)

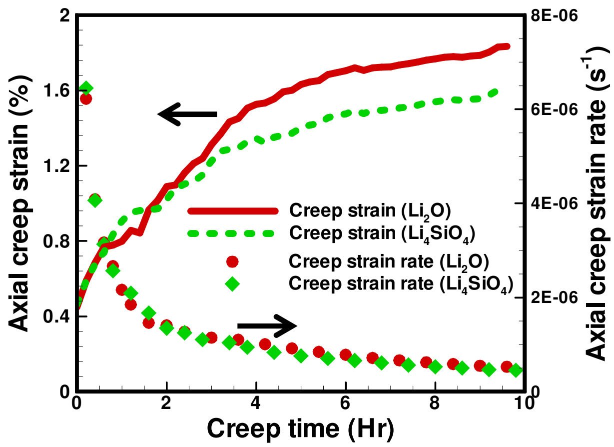

Figure 5 Axial creep strain and strain rate of Li_4SiO_4 and Li_2O pebble beds under uniaxial pressure (P = 10MPa).